THE ASTROPHYSICAL JOURNAL, 409:199–204, 1993 May 20

THE GALACTIC HALO AND LOCAL INTERGALACTIC MEDIUM TOWARD PKS 2155−304

FREDERICK C. BRUHWEILER,[1] A. BOGGESS,[2,3] DARA J. NORMAN,[4] C. A. GRADY,[1]
C. MEGAN URRY,[5] AND YOJI KONDO[6]

Received 1992 June 22; accepted 1992 November 13

ABSTRACT

The first *HST* GHRS spectra of the bright BL Lacertae object PKS 2155−304, acquired using the G140L configuration, show a smooth, featureless continuum with superposed sharp absorption. This absorption is due to both gas in the Galactic halo above the south Galactic pole and what are identified as five to six low redshift Lyα absorption systems arising in the local intergalactic medium. Complex absorption features of C IV indicate highly ionized gas at near zero velocity and ≈ -260 km s^{-1} falling toward the Galactic plane. The identified Lyα systems cover a range of redshift $0.057 \leq z \leq 0.107$. These observations confirm two features and rule out two others that were previously identified in summed *IUE* spectra of PKS 2155−304. The GHRS data resolve the strongest Lyα feature previously detected in the *IUE* data into three distinct components within the interval $z = 0.055$–0.057. A galaxy within 14′ in the plane of the sky to PKS 2155−304 with the same measured redshift as that of inferred Lyα absorption at $z \approx 0.017$ may indicate that this gas is associated with a galaxy cluster. The highest redshift observed Lyα system provides a lower limit to the distance of the BL Lacertae object ($z > 0.105$). This distance is consistent with the approximate redshift deduced from CCD imagery of the probable host galaxy for PKS 2155−304 ($z \sim 0.12$). The Lyα systems seen toward PKS 2155−304 are compared to those in the line of sight to 3C 273. A two-point correlation analysis shows no statistical evidence of clustering of Lyα features. However, apparent redshift correlations with galaxies along the line of sight argue that some significant fraction of the observed Lyα systems are associated with galaxies or galaxy clusters.

Subject headings: BL Lacertae objects: individual (PKS 2155−304) — Galaxy: halo — intergalactic medium — quasars: absorption lines

1. INTRODUCTION

Recent spectrographic results from the *Hubble Space Telescope* for line of sight toward the nearby QSO, 3C 273, have revealed as many as 16 absorption features presumably arising from redshifted H I–Lyα in a local intergalactic medium. (Morris et al. 1991; Bahcall et al. 1991). The unexpectedly large number of these low-redshift features seen in the UV and their relation to similar features of the Lyα forest at higher redshift seen at optical wavelengths have not yet been explained. Ultraviolet spectra obtained with the *HST* of low-redshift, bright active galactic nuclei (AGNs) offer an unprecedented opportunity to probe both the local Lyα forest and the outer Galactic halo of the Milky Way.

In this paper, we report on low-resolution ultraviolet observations using the Goddard High Resolution Spectrograph (GHRS) aboard the *HST* of the bright, low-redshift ($z \approx 0.15$), BL Lacertae object, PKS 2155−304. These observations, have been obtained at significantly better signal to noise (S/N) and resolution than that available from previous co-added *International Ultraviolet Explorer* (*IUE*) spectra (Maraschi et al. 1988). Results are presented that provide information on the number of intergalactic H I–Lyα components in the line of sight toward PKS 2155−304 and on the nature of the outer Galactic halo of our own Galaxy in a direction toward the south Galactic pole ($l^{II} = 17°$, and $b^{II} = -52°$).

2. OBSERVATIONS AND DATA REDUCTION

Two ultraviolet spectra of PKS 2155−304 (67 m exposures) as well as accompanying wavelength calibrations, were acquired on 1991 April 13 (UT) using the G140L low-resolution ($R = 2000$) grating configuration (not currently available) of the GHRS. The two spectra were centered at 1313 and 1585 Å and spanned the wavelength range 1165–1723 Å. Both the target acquisition and spectral data collection were performed through the square ($2'' \times 2''$) Large Science Aperture (LSA). Although the use of the LSA ensures the highest flux throughput, there is some degradation of the intrinsic spectral resolution ($\sim$0.5 Å) due to the spherical aberration of the primary mirror (Burrows et al. 1991). For both observations, the wavelength scale was derived from internal Pt-Ne lamp spectra centered at 1412.7 Å, the standard calibration wavelength for the G140L, obtained immediately prior to each observation. These calibration spectra assure a wavelength accuracy better than 1 diode, or 0.57 Å for the G140L spectral data. Both spectra of PKS 2155−304 were obtained using substep pattern 4 and the FP-SPLIT option. This set-up yielded two data points per nominal 1 diode resolution element and a means to identify non-Poisson noise and radiation events in the detector. (See Duncan & Ebbets [1989] for description of the GHRS.) The resulting subexposures for each spectrum were aligned and summed to produce the final spectra.

[1] Astrophysics Program, Department of Physics, Catholic University of America, Washington, DC 20064.
[2] Goddard High-Resolution Spectrograph (GHRS) Instrument Definition Team.
[3] Code 440, NASA/GSFC, Greenbelt, MD 20771.
[4] Member of GHRS Science Support Group/CSC.
[5] Space Telescope Science Institute, 3700 San Martin Drive, Baltimore, MD 21218.
[6] Code 684, NASA/GSFC, Greenbelt, MD 20771.

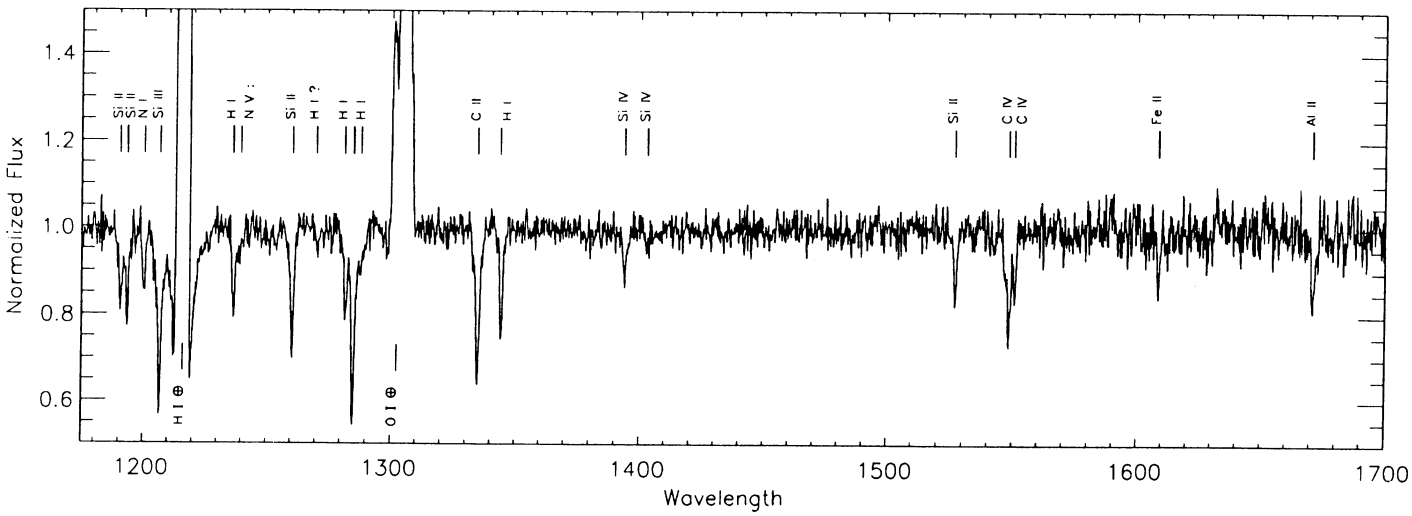

FIG. 1.—The complete normalized and merged GHRS spectrum for PKS 2155−304 is shown. The terrestial H II and O I emission features are indicated below the trace of the spectrum. Interstellar features and redshifted H I Lyα features are denoted above the spectrum. The wavelength scale is in angstroms and is in the observed frame.

An examination of the data revealed a drop of 7.5% in the continuum flux level between the short- and long-wavelength spectra. This was not due to any intrinsic flux flux variability of PKS 2155−304 between the two exposures, but to a thermal drift that caused the long-wavelength spectrum to not be properly centered upon the Digicon array. We corrected for this drift in our final resultant spectra.

Since the GHRS observations were acquired in both day and night portions of the *HST* orbit, they show contributions of geocoronal airglow emission. Both emission from H I–Lyα and the O I UV2 triplet at 1304 Å are present (Fig. 1). There is no hint of N I UV1 triplet emission at 1200 Å. The spectral region affected by O I airglow shows little or no contamination during night-time, but too few data are available from this part of the orbit to us to determine the PKS 2155−304 spectrum underlying the O I airglow emission.

After correcting for thermal drifts and accounting for terrestrial emission, the GHRS data reveal a smooth featureless continuum with the absence of any recognizable spectral emission features. The only variations from a smooth continuum, other than the sharp interstellar and intergalactic absorption features, are a broad, shallow depression $\approx$100 Å wide near 1450 Å and a large pronounced steepening of the spectral slope shortward of 1200 Å. Both of these features can be traced to inaccuracies in the fundamental UV absolute flux calibration derived from other space experiments (cf. Finley, Basri, & Bowyer 1991). Allowing for these errors in the absolute flux calibration, the intrinsic continuum of PKS 2155−304 is consistent with a featureless power-law source and a BL Lacertae object (Bregman, Maraschi, & Urry 1987). Our deduced slope for the UV power-law slope is $\alpha = -0.68 \pm 0.10$, which is consistent with previous *IUE* results (Urry et al. 1988).

The signal-to-noise ratio (S/N) per data point at the continuum for the short-wavelength observation is between 42 and 52, with the peak S/N near 1365 Å. The long-wavelength spectrum, which samples a region of lower sensitivity for the G140L, has S/N ranging from 36 at shorter wavelengths to 20 near 1720 Å.

The remainder of this paper is devoted to an analysis of the sharp absorption-line spectrum. To aid in our study of the absorption lines, the spectral data were normalized to the local continuum determined from line-free portions of the spectrum (Fig. 1). This also facilitated the subsequent analysis interpretation as discussed below.

In an attempt to recover some of the spectral resolution lost by the use of the LSA, we have applied various deconvolution techniques to the data. We have used the Jansson (1984), Richardson-Lucy (Richardson 1972; Lucy 1974), and constrained block-iterative (Heap & Lindler 1987) approaches. In all cases, we adopted a model line-spread function derived from the *HST* Faint Object Camera (FOC) F140M calibration data. These data are identical to those used by Morris et al. (1991) in their analysis of 3C 273. The Richardson-Lucy and block-iterative algorithms give similar results, with some sharpening of absorption features and a general increase in the overall noise level. Extreme care must be exercised when using the Jansson technique with its imposed constraints, especially on noisy data, since it can produce both sharp artificial absorption features and an artificially smooth continuum.

We used both the continuum normalized spectrum and the Jansson-deconvolved data to identify absorption features in the spectrum of PKS 2155−304. The previous work of Morris et al. (1991) has already shown that the deconvolved data can be a very useful tool for detecting line absorption. We have also found such data to be quite valuable in separating contributions of blended absorption features. The continuum-normalized, deconvolved data for the 1220–1350 Å region are shown in Figure 2.

3. IDENTIFIED ABSORPTION FEATURES

We measured equivalent widths for all putative features with peak absorption at least 2 σ below the local adopted continuum level. Definite identifications required that the equivalent widths be at least a 3 σ detection, plus these features must be evident in the unconvolved normalized spectrum. Weaker features, which had equivalent widths 2–3 σ above the noise limit, in the absence of other distinguishing criteria, are considered as probable detections. The pertinent data for the identified absorption features are given in Table 1. The velocity informa-

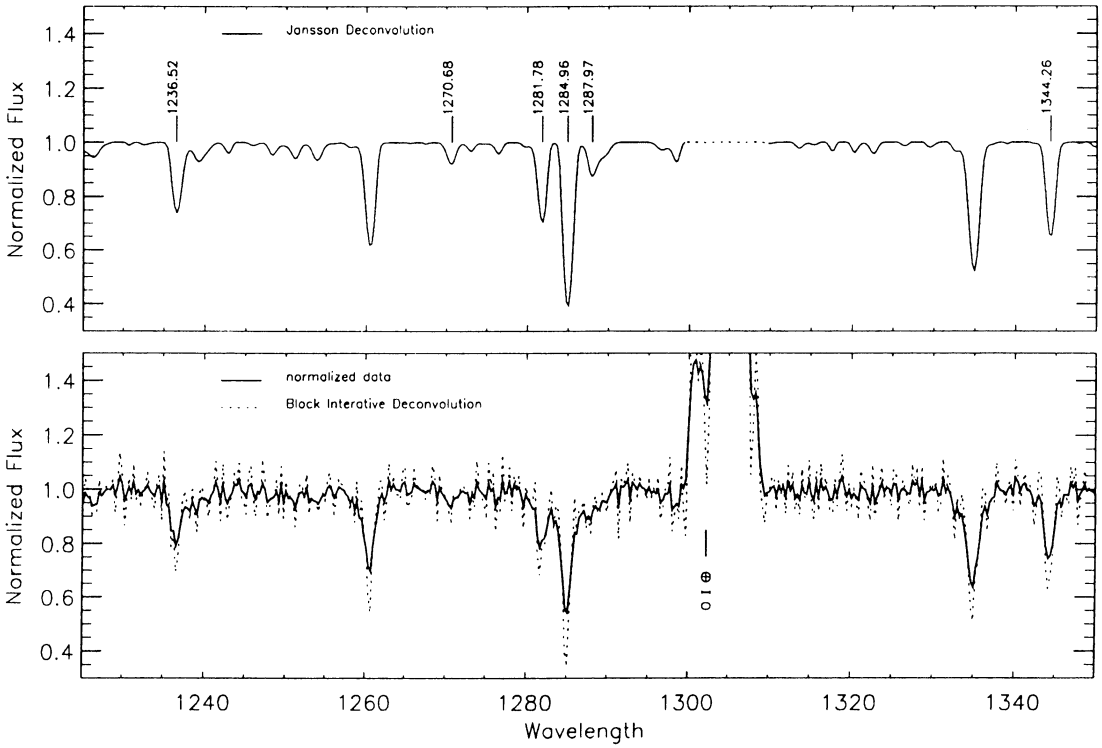

FIG. 2.—A comparison of the Jansson and Block Iterative deconvolution schemes with the normalized unconvolved data is presented. The Jansson scheme (*top panel*) is constrained an gives and artificially smooth continuum. Most of the weaker features are likely not real. The Block Iterative scheme (*bottom panel*) produces sharper features, but amplifies the noise in the data.

tion and deduced column density ranges, assuming the observed features lie on the linear and damped portions of the curve of growth, are derived based upon atomic data from the recent compilation of Morton (1991).

A total of 17 distinct features, including four blends (representing 20 individual components), met our above criteria for definite detection. Eight of the isolated lines coincide in wavelength to interstellar lines expected to be produced in the Galactic halo. Two additional isolated features were marginally detected in our spectra at 1402.78 and 1608.87 Å, but are considered as definite detections. The first feature, based on the presence of strong Si IV 1393.77 Å line, must be present and due to the weaker component of the Si IV resonance doublet. The second feature, which is a 2.5 σ detection, coincides closely with the expected interstellar Fe II 1608.79 Å. An isolated line at 1270.68 Å (2.0 σ) does not correspond to any interstellar feature expected to be found in the Galactic halo gas. Thus, it represents a possible detection of an another Lyα absorption system.

We have attempted to use the Jansson-deconvolved data to separate the identifiable components in the four blends. The 1190–1193 Å feature resolved in the original data are two distinct absorption lines in the deconvolved data set. These lines are definitely identified as Si II 1190.4 and 1193.3 Å and are expected to be formed in the halo. The 1281–1290 Å blend is resolved into three components at 1281.78, 1284.96, and 1287.97 Å. None of these wavelengths correspond to anticipated interstellar features in the halo. Discussion of the complex absorption features at 1236–1240 Å and 1545–1551 Å are presented below.

In Table 1, 14 of the 20 listed lines can be identified unambiguously with interstellar galactic halo gas. All of these lines have been routinely seen in *IUE* data. For these lines, column (10) gives the deduced radial velocity range in the deconvolved data set. For all Galactic halo absorption features, except that for C IV, the GHRS G140L data indicate gas only near zero velocity.

4. GALACTIC HALO TOWARD PKS 2155−304

The line of sight toward PKS 2155−304 ($l^{II} = 17°$, and $b^{II} = -52°$) is in the direction of the south Galactic pole. The GHRS data, as presented in Table 1, indicate definite detections of the expected interstellar features of Si II, Si III, Si IV, C IV, and Al II. Only Fe II 1608 Å lies below our 3 σ detection criterion.

We have used the zero-velocity H I interstellar absorption to derive the H I column density through the halo. A fit to the damping wings of the Lyα profile yields N(H I) = 1.0 ± 0.2 × 10^{20} cm^{-2}, using both the block-iteratively deconvolved data and the continuum normalized data. Both the 21 cm surveys of Stark et al. (1992) and Heiles & Cleary (1983) indicate N(H I) = 1.8 × 10^{20} cm^{-2} in this direction. However, the emission line results cannot be directly compared to absorption line results due to the finite beam size in these studies (i.e., ≈2° for Stark et al.). Yet, similar profile fitting for H I in *IUE* data for HD 204076, a B1 V star at a distance of 1.7 kpc at $l^{II} = 14°$, $b^{II} = -46°$, yields N(H I) = 5 × 10^{20} cm^{-2} (Savage & Massa 1987). A comparison of all these results and the "apparent" uniformity of the low-level 21 cm emission in the Stark et al. maps in this direction implies that these variations

TABLE 1

ABSORPTION LINES IN THE GHRS SPECTRUM OF PKS 2155−304

MEASUREMENTS			IDENTIFICATION		COLUMN DENSITIES[c]		VELOCITY	
λ_{obs}[a] (Å)	EW (mÅ)	σ_{EW} (mÅ)	ION	λ_{lab}[b] (Å)	log (N_{min}) (cm^{-2})	log (N_{max}) (cm^{-2})	v_{cen} or (z)	FWHM[d] (km s^{-1})
1190.72	280[e]	56	Si II	1190.42	13.93	16.69	+76	390
1193.46	266[e]	56	Si II	1193.29	13.62	16.34	+43	280
1200.27	250	50	N I	1200.01[f]	13.87	17.47	+65	440
1206.65	730	48	Si III	1206.50	13.52	16.80	+37	410
1215.67	...	...	H I	1215.67	19.90[g]	20.08	0:	...
1236.52	480	43	H I	1215.67	13.94:[d]	17.63:[d]	(0.017)	360
1260.44	480	42	Si II	1260.42	13.52	16.57	+5	370
1270.68:	82:	40	H I	1215.67	...	...	(0.045)	...[h]
1281.78	350[e]	40	H I	1215.67	13.78	17.32	(0.055)	360
1284.96	810[e]	40	H I	1215.67	14.14	18.05	(0.057)	370
1287.97	230[e]	40	H I	1215.67	13.60	16.95	(0.059)	620:
1334.93	800	40	C II	1335.08[f]	14.13:	18.35:	−34:	420
1344.26	390	40	H I	1215.67	13.81	17.38	(0.105)	340
1393.80	260	42	Si IV	1393.76	13.53	16.74	+9	310
1402.78	120	42	Si IV	1402.77	13.48	16.38	+2	370:
1527.13	300	57	Si II	1526.71	13.80	16.60	+83	230
1546.8	170[e]	59	C IV	1548.20	13.62	17.03	−260:	355:
1548.20:	310[e]	59	C IV	...[i]	...	...	+32	330:
1550.87	230[e]	59	C IV	1550.77	14.05	17.59	+19	380
1608.78	190	77	Fe II	1608.45	14.12	17.6	+61	210
1671.16	320	83	Al II	1670.79	12.85	15.72	+66	290

[a] Observed wavelengths measured from data deconvolved using the Jansson 1984 algorithm.

[b] Laboratory wavelengths from Morton 1991.

[c] The column densities ranges are calculated assuming the observed features either fall on the linear or damped portion of the curve of growth.

[d] W_λ and N(H I) highly uncertain. Low-velocity, weak N V $\lambda\lambda$1238.82, 1242.80 may be present and blended with H I.

[e] Observed equivalent width measured from deconvolved data due to blending with nearby line(s). The full-width full maximum of the blend representing the redshifted H I complex near 1280 Å is 10 Å in the unconvolved data.

[f] Laboratory wavelength is weighted average of several lines from multiplet which are blended at the resolution of the GHRS G140L. Thus, values for v_{cen} and FWHM are less reliable. Highly inaccurate for C II, since 1334 and 1335 Å transitions arise from two distinct J-levels.

[g] Galactic H I column density calculated by fitting the wings of Lyα which were fully resolved in the GHRS G140L data.

[h] Inferred column densities of 1270.68 Å not given due to the uncertainty of detection.

[i] Blend of two C IV lines, 1548.20 near zero velocity and 1550.77 Å near −260 km s^{-1}.

must be due to small-scale spatial structure at scales smaller than 2° on the plane of the sky.

The low-ionization species, as well as Si III and Si IV, in the halo show no evidence of high-velocity components. The detected features of C II, N I, Si II, and Fe II, all indicate velocities $\leq$100 km s^{-1}. The strength of this absorption is consistent with that found in the survey of the inner halo by Danly (1989).

The high ionization C IV presents evidence of both low- and high-velocity absorption. The G140L data clearly resolve both members of the resonance doublet at $\lambda\lambda$1548.2, 1550.8. However, the data show a shallow shortward-displaced component extending from the shortward component of the doublet (See Fig. 3). A multiple Gaussian fit to the data, modeling both members of the doublet, indicates C IV near 0 and −265 km s^{-1}. Nonetheless, we cannot eliminate the possibility of C IV absorption over a range of smaller, negative velocities. No high-velocity N V or Si IV mirroring that of C IV is seen. The presence of infalling highly ionized C IV in the halo and constraints on Si IV and N V are consistent with galactic fountain models (Bregman 1987) where the absorption is produced in cooling plasma ($T \approx 5 \times 10^4$ K) falling toward the Galactic plane. Data for additional lines of sight toward the SGP are needed to confirm and map out the spatial extent of this gas.

The ion, N V, has been observed in the Galactic halo toward 3C 273 (Morris et al. 1991; Bahcall et al. 1991) and the close coincidence of the features at $\lambda\lambda$1236−1240 with N V is very suggestive (Fig. 2). However, careful examination shows little or no contributing N V. The observed feature exhibits strong absorption at 1236.5 Å with a shallow, longward extending wing. If the 1236.5 Å were the stronger member of the N V doublet displaced −560 km s^{-1}, then the weaker member of the doublet should produce a corresponding strong absorption of at least $\frac{1}{2}$ the equivalent width centered at 1240.5 Å. The weak absorption at that wavelength is far less than that expected for N V. We must conclude that, if N V is present, it comprises only a minor fraction of the observed $\lambda\lambda$1236–1242 absorption. We identify the main component of this absorption centered at 1236.5 Å as redshifted Lyα at $z = 0.017$. The longer wavelength absorption wing may be either undisplaced N V or additional Lyα at slightly higher z. The entirety of this feature may be all due to redshifted Lyα. Extreme equivalent width upper limits for the undisplaced N V doublet are 136 and 68 mÅ.

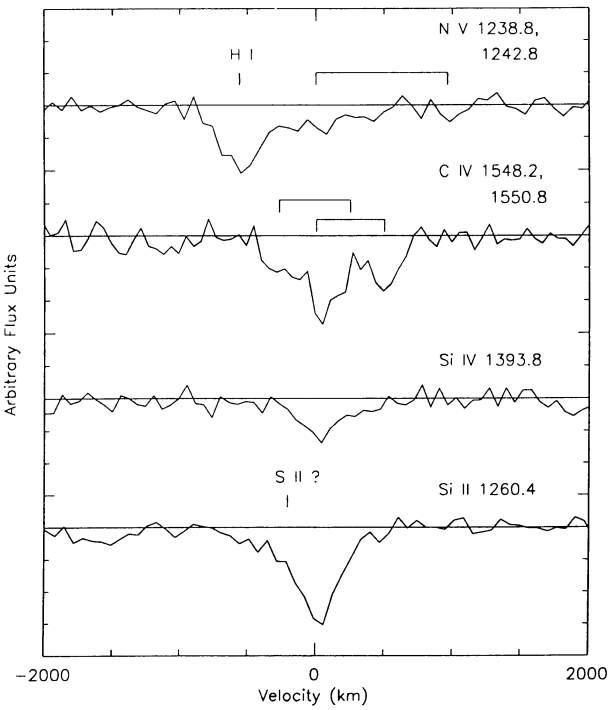

FIG. 3.—Four spectral regions are shown mapped in velocity space that correspond to both low- and high-ionization species in the halo. The velocity mapping was done for the lines N V λ1238.821, C IV λ1548.195, Si IV λ1393.755, and Si II λ1260.421 from the top to bottom panels, respectively. Most, possibly all, of the absorption in the N V region is due to redshifted H I Lyα (see text). Absorption from both members of the C IV doublet is seen. Plus, C IV at −260 km^{-1} is indicated. The shortward wing of the Si II λ1260.421 is likely from S II λ1259.53 in the galactic halo.

5. Lyα COLUMN DENSITIES AND THE SEARCH FOR INTERGALACTIC METALLIC LINES

Our data are consistent with the detection of five Lyα features and marginal detection of one additional system (2.0 σ) with redshifts $0.0168 \leq z \leq 0.105$. Four Lyα systems have $W_\lambda \approx 250$ mÅ, comparable to the strongest Lyα systems detected toward 3C 273 (Morris et al. 1991; Bahcall et al. 1991), while the strongest system at 1284.96 Å, has an equivalent width 3–4 times larger (See Table 1).

The implied H I column densities are ill-defined. There has been a great deal of discussion about what b-values are appropriate for Lyα systems, where the instrumental resolution usually defines the upper limit to b [and a lower limit to N(H I)]. Recent ground-based observations (Pettini et al. 1990) at 6.5 km s^{-1} resolution for Lyα systems with $z = 2.1$–2.6 have indicated generally that $b \leq 22$ km s^{-1}. Because of the low resolution of the GHRS data, only very weak constraints can be imposed upon the H I column densities. These come from the linear and damping asymptotic limits of the curve-of-growth. These limits upon N(H I) are given in Table 1.

If the H I column density, especially for the strongest Lyα system at 1284 Å, is near the derived upper limit, then absorption from heavy elements might be seen at this same redshift. If comparison can be made with optical Lyα systems, absorption in metals, particularly in C IV, should be easily detectable in data presented here. High-redshift Lyα systems have typical C IV equivalent widths which are $\approx\frac{1}{3}$ of the Lyα equivalent width (Sargent, Boksenberg, & Steidel 1988), implying $W_\lambda \approx$ 220 mÅ. We find no detectable C IV absorption at $z = 0.057$ (1637 Å) with an upper limit of 110 mÅ, or at any other wavelength corresponding to redshifts of our identified Lyα systems. Similarly, no redshifted features of low-ionization species such as Si II λ1260, O I λ1302, and C II λ1334 can be identified with upper limits $\lesssim$90 mÅ. The only coincidence that can be found is for a 1.4 σ feature at 1276.2 Å, which would be redshifted Si III 1206.5 Å at $z = 0.057$. Based upon the S/N statistics, we must conclude that this feature is likely not real and the wavelength coincidence is merely fortuitous.

We must mention that we find no absorption due to either N V or C IV that might be associated with the X-ray trough seen near 600 eV in PKS 2155−304 (Canazares & Kruper 1984; Urry, Mushotsky, & Holt 1986) that has been attributed to Lyα K-shell resonance absorption from O VIII. If we assume that absorption from these ions originate in PKS 2155−304 at a redshift of $z = 0.117$ as inferred by Bowyer et al. (1984), then N V and C IV absorption would be seen at 1385 and 1730 Å. Our data can only sample N V at this redshift and sets an upper limit of 41 mÅ for redshifted N V λλ1238, 1242. Since the ionization of O VIII requires energies well beyond those required for C IV and N V, the absence of C IV and N V should not be surprising. Thus, one possible interpretation is that the N V and C IV are not produced in the same region as O VIII.

6. NATURE OF THE REDSHIFTED Lyα SYSTEMS

Our GHRS observations of PKS 2155−304 reveal five, possibly six, features that can be identified as absorption arising in a local H I Lyα forest within a redshift range $0.017 \leq z \leq 0.105$. This likely denotes a complete sample for $W_\lambda \geq 160$–180 mÅ. This is comparable to the six redshifted Lyα features identified in the FOS spectra of 3C 273 for a comparable redshift range and equivalent width detection limit (Bahcall et al. 1991). However, as shown in Morris et al. (1991), the GHRS/G160M observations with a detection limit of $W_\lambda \approx 25$ mÅ revealed a total of 16 redshifted components.

Noteworthy in the GHRS observations of PKS 2155−304 is the complex of three very strong lines (see Table 1) spanning the narrow redshift range 0.053–0.057 seen at 1281–1288 Å. The only strong lines in 3C 273 exhibiting similar close wavelength (redshift) spacing are those at 1219.8 (371 mÅ) and 1222.12 (410 mÅ), implying $z = 0.0036$ and 0.0057, respectively. Bahcall et al. suggest that these two strong features are associated with the nearby Virgo Cluster, possibly arising in the halos of intervening galaxies. The implied redshifts of the three-lined complex in PKS 2155−304 is much higher, but could originate in a more distant, yet unrecognized galaxy cluster in the line of sight toward PKS 2155−304.

In an attempt to investigate further the correlation of Lyα absorption with galaxy clusters toward PKS 2155−304, we used the IPAC extragalactic data base to search for redshift coincidences between foreground galaxies and candidate redshifted Lyα features in PKS 2155−304. The closest galaxy in the plane of the sky with a measured radial velocity is ESO 215709−3025.5, which lies 14.′6 away. Data from the IPAC data base indicate this galaxy is a 1.′4 diameter Sb-type spiral galaxy with an $m_v = 14.39$. Its redshift, $z = 0.017$, is in excellent agreement with the deduced Lyα absorption at 1236.5 Å. The implied distance of the Lyα cloud from the spiral galaxy is $\approx$400 kpc—for $H_0 = 50$ km s^{-1} Mpc^{-1}, which indicates that it can be associated with the galaxy cluster containing ESO 215709−3025.5, but probably not associated with the specific galaxy.

Additional investigation shows that the Abell cluster 3832−3 (actually one cluster) centered at $\alpha = 22^h02^m.4$; $\delta = -30°43'$ lies along the sightline toward PKS 2155−304. There are no measured radial velocities for any "confirmed" members of the cluster, but the inferred redshift based upon the 10th brightest galaxy of the cluster (Abell, Corwin, & Olowin 1989) gives $z = 0.107$ with an associated error of a factor of 2, and thus consistent with the redshift (0.105) of the 1344 Å feature seen in the GHRS spectrum. Certainly, future ground-based radial velocity determinations will be able to determine a more accurate value for the redshifts of galaxy members of A3832−3.

Recent high-resolution imaging of PKS 2155−304 is consistent with the AGN being embedded in a giant elliptical galaxy at $z \approx 0.1$ (Falomo et al. 1991). Moreover, the field around PKS 2155−304 shows numerous galaxies with two having measured redshifts of 0.116 and 0.117 (Also see Bowyer et al. 1984). Falomo et al. also mention a hint of absorption features at $z \approx 0.1$ in spectra sampling the candidate host galaxy of PKS 2155−304 at 5″ away from the nucleus. However, if this galaxy and the surrounding galaxies are members of the same cluster, they should all have $z \approx 0.117 \pm 0.002$. If so, this implies that the 1344 Å Lyα feature originates in the foreground to these galaxies. It still remains to be determined if these galaxies are associated with A 3822−3 or denote a separate group.

It is important to determine the degree of evolution of the Lyα systems as a function of redshift. We can represent the number density of Lyα lines versus redshift by $dN/dz \propto (1 + z)^\gamma$. A comparison of results for $z \approx 0$, including PKS 2155−304, and for high z (Weyman 1991) show a much flatter slope at low z. For low z and $W_\lambda \geq 200$ mÅ, Weyman finds $\gamma = 0.54$. If the contributions of the two clouds seen toward 3C 273 thought to be associated with the Virgo Cluster are removed, γ becomes 0.83. The values for γ are much larger for the sample with $z \geq 2.0$. For example, the data by Lu, Wolfe, & Turnshek (1991) indicate $\gamma = 2.75 \pm 0.29$ (See Weyman 1991 for additional discussion.) It is not clear if this change in slope reflects a significant change in the evolution of these clouds, or if the Lyα systems at $z \approx 0$ seen by the *HST* typify a different cloud population than that at high z.

How strong is the evidence for clustering in the low-redshift Lyα systems? If the data for 3C 273 and PKS 2155−304 are combined, excluding the absorption likely produced in the nearby Virgo Cluster, we find a total of 10 ordered pairs of lines out of a total of 17 with redshift separations less than 0.005. This compares with a mean separation for neighboring components of 0.0126. At first glance this seems to suggest some degree of clustering in the local Lyα forest. Yet this conclusion is not supported in a two-point correlation analysis which uses all possible pairs of lines in the observed sample. For the common redshift range over which the candidate Lyα absorption has been detected (0.0218–0.105), after correcting for the fact that a finite bandwidth permits more complete sampling of smaller separations than larger ones (Sargent et al. 1980), the assumption of Poisson statistics suggests that each bin of width $\Delta z = 0.005$ should have 13.8 ± 3.7 components versus the observed 10. Thus, there is no statistical evidence for clustering of Lyα forest lines as a whole. However, the existence of 1219 and 1222 Å features in 3C 273, together with the three closely spaced lines near 1238 Å and the close proximity of a galaxy to another of the lines in PKS 2155−304, constitutes persuasive evidence that at least a significance fraction of the low-redshift Lyα systems are associated with galaxies or galaxy clusters. More definite conclusions must await further UV spectral observation of other low-redshift AGNs and subsequent studies of foreground galaxies and clusters in the fields toward these objects.

REFERENCES

Abell, G. O., Corwin, H. G., & Olowin, R. P. 1989, ApJS, 70, 1
Bahcall, J. N., Jannuzi, B. T., Schneider, D. P., Hartig, G. F., Bohlin, R., & Junkkarinen, V. 1991, ApJ, 377, L5
Bowyer, S., Brodie, J., Clarke, J. T., & Henry, J. P. 1984, ApJ, 287, 845
Bregman, J. N., Maraschi, L., & Urry, C. M. 1987, in Exploring the Universe with the *IUE* Satellite, ed. Y. Kondo (Dordrecht: Reidel), 685
Burrows, C. J., Holtzman, J. A., Faber, S. M., Bely, P. Y., Hasan, H., Lynds, C. R., & Schroeder, D. 1991, ApJ, 369, L21
Canizares, C. R., & Kruper, J. 1984, ApJ, 278, L99
Danly, L. 1989, ApJ, 342, 785
Duncan, D. K., & Ebbets, D. 1990, GHRS Handbook V.2.0 (Baltimore: STScI)
Falomo, R., Giraud, E., Maraschi, L., Melnick, J., Tanzi, E. G., & Treves, A. 1991, ApJ, 380, L67
Finley, D. S., Basri, G., & Bowyer, S. 1990, ApJ, 359, 483
Heap, S., & Lindler, D. 1987, A&A, 115, L10
Heiles, C., & Cleary, M. N. 1967, Australian J. Phys. Suppl., 47, 1
Jansson, P. A. 1984, Deconvolution with Applications in Spectroscopy (New York: Academic)
Lu, L., Wolfe, A. M., & Turnshek, D. A. 1991, ApJ, 367, 19
Lucy, L. B. 1974, AJ, 79, 745
Maraschi, L., Blades, J. C., Calanchi, C., Tanzi, E. G., & Treves, A. 1988, ApJ, 333, 660
Morris, S. L., Weymann, R. J., Savage, B. D., & Gilliland, R. L. 1991, ApJ, 377, L21
Morton, D. C. 1991, ApJS, 77, 119
Pettini, M., Hunstead, R. W., Smith, L., & Mar, D. P. 1990, MNRAS, 246, 545
Richardson, W. H. 1972, J. Opt. Soc. Am., 62, 55
Sargent, W. L. W., Boksenberg, A., & Steidel, C. C. 1988, ApJS, 68, 539
Sargent, W. L. W., Young, P. J., Boksenberg, A., & Tytler, D. 1980, ApJS, 42, 41
Savage, B., & Massa, D. 1987, ApJ, 314, 380
Stark, A. N., et al. 1991, ApJS, 79, 77
Urry, C. M., Kondo, Y., Hackney, K. R. H., & Hackney, R. L. 1988, ApJ, 330, 791
Urry, C. M., Mushotzsky, R. F., & Holt, S. S. 1986, ApJ, 305, 369
Weyman, R. J. 1991, in The First Year of *HST* Observations, ed. A. Kinney & J. C. Blades (Baltimore: STScI), 58